JOURNAL OF SOLID STATE CHEMISTRY **133,** 5–10 (1997)
ARTICLE NO. SC977306

The Effect of Pd, Pt, and Co on the Superconducting and Magnetic Ordering Temperatures in RNi$_2$B$_2$C (R = Tm and Er)

I. Felner,* D. Schmitt,† B. Barbara,† C. Godart,‡ and E. Alleno‡

*Racah Institute of Physics, The Hebrew University, Jerusalem 91904, Israel; †Laboratoire de Magnetisme L. Neel, 38042 Grenoble Cedex 9, France; and ‡Chimie Metallurgique et Spectroscopie des Terres Rares, CNRS, Place Aristide Briand, 92195 Meudon Cedex, France, and LURE, CNRS, Universite de Paris Sud, 91405 Orsay Cedex, France

Received January 21, 1997; accepted February 6, 1997

We have investigated the nearly isotropic superconducting intermetallic RNi$_{2-x}M_x$B$_2$C system (M = Pd, Pt, and Co, x = 0.05−0.2) by complementary experimental techniques. For TmNi$_2$B$_2$C, T_C = 10.7 K and the antiferromagnetic (AFM) order of the Tm spins develops below T_N = 1.48 K. Pt as a dopant affects T_C very little, whereas, for M = Pd, T_C is reduced to 9.9 and 9.1 K for x = 0.05 and 0.1, respectively. For TmNi$_2$B$_2$C and TmNi$_{1.9}$Pt$_{0.1}$B$_2$C, the H_{c1} values exhibit a maximum at 3 K. While the AFM transition for TmNi$_2$B$_2$C at T_N is clearly identified by specific heat measurements, no specific heat anomaly was observed for TmNi$_{1.9}$Pd$_{0.1}$B$_2$C down to 0.8 K, indicating that Pd as a dopant drastically reduces T_C and T_N of the system. For ErNi$_2$B$_2$C, T_C = 10.9 K and T_N = 6.3 K ($T_C > T_N$). In ErNi$_{2-x}M_x$B$_2$C, both Pt and Pd as dopants (x = 0.2) reduce T_C to ~8 K and shift T_N to ~11 K. For M = Co and x = 0.05 T_C is reduced to 4.8 K and T_N increases to 8.2 K. For higher Co concentrations (x = 0.2 and 0.5), the compounds are not superconducting, and T_N increases to 10.9 and 14.8 K respectively. It appears that for ErNi$_{2-x}M_x$B$_2$C (i) for x = 0.2 the same T_N ~11.K is obtained regardless of M, and that (ii) in contrast to R = Tm, all dopants studied lead to a reduction of T_C and to an increase of T_N of the Er sublattice, thus $T_C < T_N$. The delicate interplay between superconductivity and AFM in this system is discussed. © 1997 Academic Press

1. INTRODUCTION

The discovery of superconductivity (SC) in RNi$_2$B$_2$C (R = rare-earth) (1–4) and other quaternary lanthanide transition-metal borocarbides with critical temperatures T_C up to 23 K (5) has received great attention because some members of the series with magnetic rare earths, R = Dy, Ho, Er, and Tm, are antiferromagnetically (AFM) ordered at low temperatures. These compounds crystallize in a filled version of the body-centered tetragonal $ThCr_2Si_2$ type structure, stabilized by the incorporation of carbon in the R planes which separate the Ni_2B_2 layers.

Competition between SC and magnetism has been one of the main topics of study in the field of SC research. The striking features of RNi$_2$B$_2$C magnetic superconductors, which distinguish them from all other known magnetic superconductors including high T_C superconductors, are (1) their relatively high T_C values (16.2 K for R = Lu) and (2) their relatively high AFM temperature transitions (T_N) values (T_N = 10.3 K for R = Dy). In Fig. 1, several T_C and T_N values are plotted as a function of the de Gennes factor (DG = $(g-1)^2J(J+1)$ normalized to DG = 1 for Gd), demonstrating that the decrease of T_C and the increase of T_N roughly scales by DG. This shows the strong correlation between SC and T_N values and gives evidence for the dominance of the magnetic pair-breaking effect in the systematic change of T_C with R element. It is readily observed, that for R = Ho, Er, and Tm, $T_C > T_N$. On the other hand, DyNi$_2$B$_2$C is an exception in which $T_N > T_C$, and the intriguing question arises as whether this observation is unique for R = Dy.

When Ni is partially replaced by a different 3d element such as Pd, Pt, or Co, T_C decreases as demonstrated for RNi$_{2-x}M_x$B$_2$C systems (6, 7). The purpose of this paper, employing several complementary experimental techniques, is to obtain information about the influence of 3d M substitution (M = Pd, Pt, and Co) on the interplay between SC (T_C) and magnetism (T_N). In order to answer the question raised above, we carried out dc and ac susceptibility measurements on the systems TmNi$_2$B$_2$C (T_C = 10.8 and T_N = 1.48 K) and ErNi$_2$B$_2$C (T_C = 10.7 and T_N = 6.3 K), and we show that their behavior is quite different. In TmNi$_{2-x}M_x$B$_2$C, Pt as a dopant affects T_C very little, whereas Pd drastically reduces both T_C and T_N, and for x = 0.1 we obtain T_C = 9.1 and T_N < 0.8 K. On the other hand, ErNi$_{2-x}M_x$B$_2$C serves as a second system in which $T_N > T_C$, because all dopants studied (M = Pd, Pt, and Co) lead to a reduction of T_C and a shift T_N of the Er sublattice to $T > T_C$.

0022-4596/97 $25.00

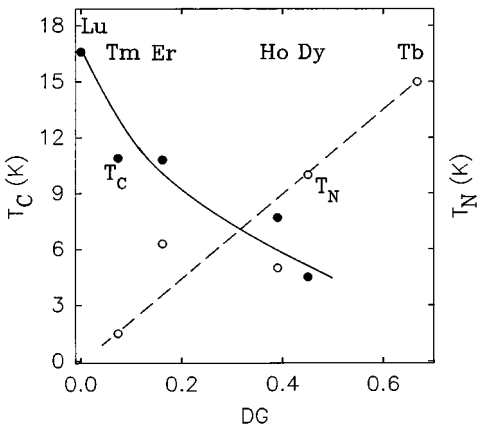

FIG. 1. The variation of T_C and T_N values as a function of the de Gennes factor normalized to Gd for the heavy $R\mathrm{Ni_2B_2C}$ system.

2. EXPERIMENTAL

The samples were prepared by arc melting the constituent elements under argon. Buttons were flipped over and melted six times to insure homogeneity. The buttons were sealed in evacuated quartz tubes and annealed at 800 C for about two weeks. Samples were characterized by powder X-ray diffraction (XRD) and the lattice parameters obtained by a least-squares fit procedure are listed in Table 1. Zero-field-cooled (ZFC) and field-cooled (FC) dc susceptibility measurements at various applied fields (H) and studies of ac susceptibility (at frequency 10 Hz and field amplitude 1 Oe) as a function of temperature were performed using a SQUID magnetometer (Quantum Design). The specific heat measurements at $H = 0$ T were carried out using the ac calorimetery technique in the temperature range 0.8–40 K. X-ray absorption spectroscopy (XAS) measurements were performed at the French synchrotron radiation facility (LURE) in Orsay, using the X-ray beam of the DCl storage ring (working at 1.85 GeV and 220 mA) on the EXAFS D21 station. Experiments were carried out in the 8600–8700 eV energy range which contain the L_{III}-edge of Tm at 300 K. The background was subtracted in a standard manner (8).

TABLE 1
Lattice Parameters, Phase Purity, and SC and AFM Transitions of $\mathrm{RNi_{2-x}}M_x\mathrm{B_2C}$

Compound	a (A°) ±0.001	c (A°) ±0.001	I_{imp}/I (as cast)	I_{imp}/I (800 C)	T_C (K) ±0.1	T_N (K) ±0.1
$TmNi_2B_2C$	3.485	10.588	0.03	—	10.7	1.5
$TmNi_{1.95}Pd_{0.05}B_2C$	3.488	10.598	0.12	0.02	9.9	
$TmNi_{1.90}Pd_{0.10}B_2C$	3.489	10.595	0.13	—	9.1	< 0.8
$TmNi_{1.95}Pt_{0.05}B_2C$	3.490	10.601	0.06	0.01	10.8	
$TmNi_{1.90}Pt_{0.10}B_2C$	3.494	10.612	0.22	0.08	10.5	
$ErNi_2B_2C$	3.502	10.563		—	10.9	6.3
$ErNi_{1.8}Pd_{0.2}B_2C$	3.513	10.584		0.07	7.9	11.1
$ErNi_{1.8}Pt_{0.2}B_2C$	3.517	10.613		0.04	8.0	11.0
$ErNi_{1.95}Co_{0.05}B_2C$	3.501	10.555		0.05	4.7	8.2
$ErNi_{1.8}Co_{0.2}B_2C$	3.499	10.534		0.02	—	10.9
$ErNi_{1.5}Co_{0.5}B_2C$	3.500	10.523		0.01	—	14.8

3. RESULTS AND DISCUSSION

A. The $TmNi_{2-x}M_xB_2C$ (M = Pd and Pt) System

The XRD patterns of samples were taken as cast, and after 14 days annealing at 900 and 800 C. In Fig. 2 diffractograms of $TmNi_{1.95}Pd_{0.05}B_2C$ show that levels of the main impurity TmB_2C_2 are smaller after annealing at 800°C. Table 1 shows the ratio between the intensity of the main XRD peak of TmB_2C_2 over the intensity of the main peak of the compound, before and after the heat treatment. All magnetic measurements on $\mathrm{TmNi_{2-x}}M_x\mathrm{B_2C}$ described below have been performed on these materials. The samples crystallize in the tetragonal $ThCr_2Si_2$ type structure, and the lattice parameters obtained are presented in Table 1. A small but significant change of the a and c lattice parameters with growth of Pd and Pt or of Co concentration indicates a steady incorporation of these elements on Ni sites. The local electronic structure of the Tm ions in $\mathrm{TmNi_{2-x}}M_x\mathrm{B_2C}$ was studied at 300 K by X-ray L_{III} edge absorption studies, and the results obtained are shown in Fig. 3. Generally speaking, all spectra show a single line at ~ 8650 eV which is attributed to Tm^{3+}, indicating that the substitution of Pd and/or Pt does affect the Tm valence.

I. The superconducting state. The ZFC and FC magnetic susceptibility curves ($\chi(T) = M/H$) measured at 20 Oe for $TmNi_2B_2C$ are shown in Fig. 4. $T_C = 10.7$ K is defined as the onset of the sharp decrease in $\chi(T)$ (Fig. 4 inset). The same criteria have been used for all $\mathrm{TmNi_{2-x}}M_x\mathrm{B_2C}$ samples, and the values obtained are listed in Table 1. It appears that Pd and Pt as dopants behave differently. Pt affects T_C very little, whereas for M = Pd, T_C varies linearly with x. For $x = 0.1$, we obtained $T_C = 9.1$ K. For all materials we measured, (1) the ZFC and FC $\chi(T)$ branches at higher applied fields as well as (2) the magnetization loops as a function of the applied field up to 5 T, at various constant temperatures. The values of the critical fields and of characteristic length scales such as the coherence and the penetration lengths as well as of different irreversibility phenomena will be published and discussed elsewhere.

From the low field part of the magnetization loops in the ZFC process measured at various temperatures, the lower critical field (H_{c1}) values can be extracted. Typical low-field $M(H)$ isotherm curves for $TmNi_2B_2C$ are shown in Fig. 5.

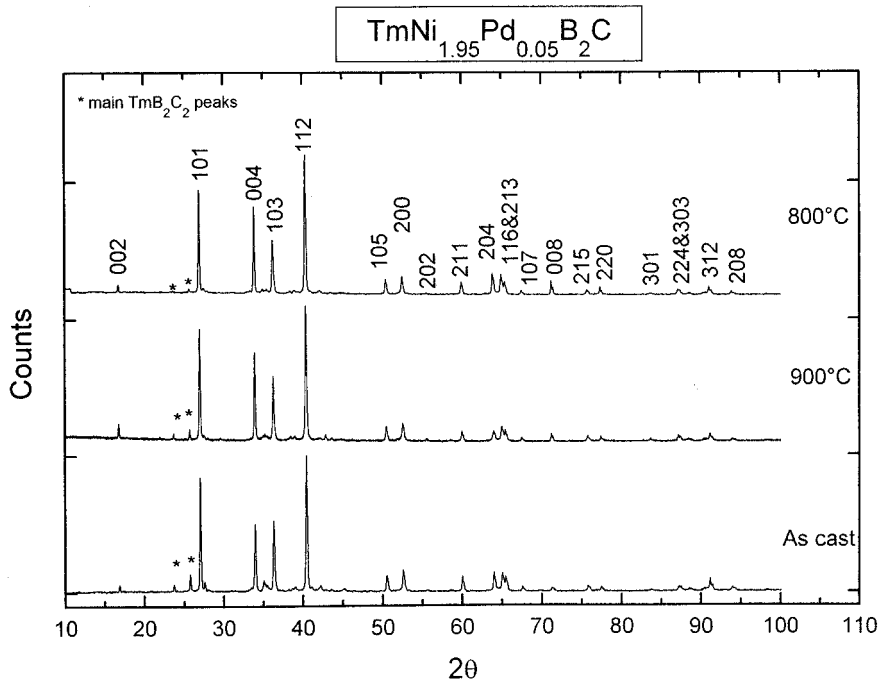

FIG. 2. X-ray diffraction patterns for $TmNi_{1.95}Pd_{0.05}B_2C$ as cast after annealing at 800 and 900 C.

Note that the curve measured at 1.8 K lies (for $H > 300$ Oe) above that obtained for $T = 3$ K. In the Meissner state (below H_{c1}), the total negative magnetic moment of a superconductor is linear with H, and given by

$$M = -H * V/4\pi(1 - N) \qquad [1]$$

where V is the volume of the sample and N is the demagnetization factor. For accurate determination of the deviation from the linear behavior we have used the parameter $p = 4\pi M/H * V = -1/(1 - N)$, which is constant up to applied field H_{c1}. Plotting the p parameter as a function of H at various temperatures, using $\Delta p = 0.05$ as a criterion for

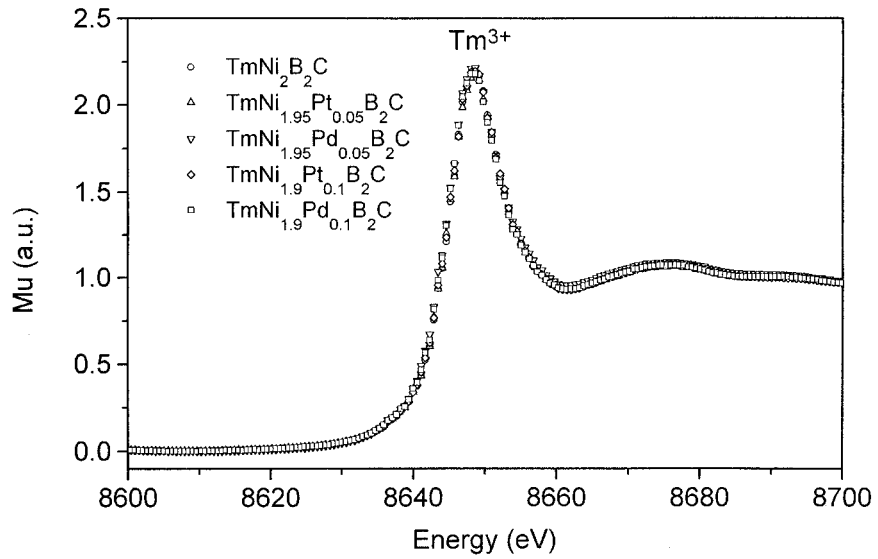

FIG. 3. X-ray absorption spectra at the TmL_{III} edge of $TmNi_{2-x}M_xB_2C$ measured at 300 K.

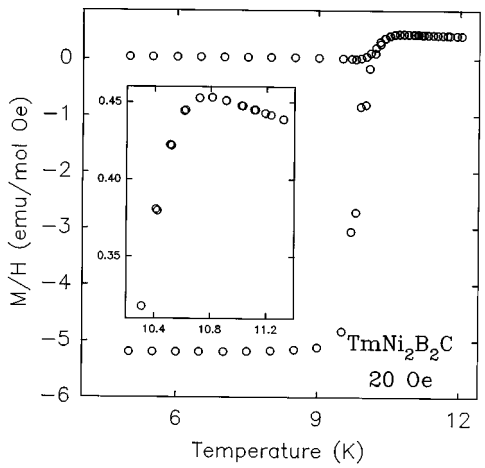

FIG. 4. ZFC and FC susceptibility measured at 20 Oe for $TmNi_2B_2C$. The SC transition range is expanded in the inset.

deviation from a constant value, we obtained $H_{c1}(T)$ within error $\Delta H_{c1} = 5$–6 Oe. The values obtained for $TmNi_2B_2C$ and $TmNi_{1.9}M_{0.1}B_2$ (M = Pt and Pd) are shown in Fig. 5 (inset). (The lines are a guide for the eyes).

Several characteristic features in $H_{c1}(T)$ of $TmNi_{1.9}M_{0.1}B_2$ can be pointed out. (1) The estimated $H_{c1}(0) \sim 400$ Oe is lower than the 800 Oe obtained for the nonmagnetic R elements, YNi_2B_2C and $LuNi_2B_2C$ (9). (2) For both $TmNi_2B_2C$ and $TmNi_{1.9}Pt_{0.1}B_2C$ samples, H_{c1} is suppressed at low temperatures as T approaches T_N (see below) with a broad maximum above T_N which is in common in antiferromagnetic superconductors (10). Thus this suppression is attributed to the interplay between the magnetism of the Tm^{3+} ions and superconductivity. It should be noted that similar behavior has been observed for the higher critical field H_{c2} of $TmNi_2B_2C$ (11). (3) For $TmNi_{1.9}Pd_{0.1}B_2C$, a conventional $H_{c1}(T)$ was observed and the experimental values fit to the empirical equation:

$$H_{c1}(T) = H_{c1}(0)[1 - (T/T_C)^2] \text{ with } H_{c1}(0) = 352 \pm 8 \text{ Oe}. \quad [2]$$

II. The Tm magnetic state. Figure 6 displays the temperature-dependent specific-heat data, $C_p(T)$ measured at $H = 0$ T, of $TmNi_2B_2C$ at $0.8\text{ K} < T < 15\text{ K}$. There is a clear lambda-shaped anomaly with a peak at $T_N = 1.477(2)$ K that can be associated with the transition of the Tm sublattice from paramagnetism to AFM order. This value is in perfect agreement with Ref. (11). Note that the SC transition at $T_C = 10.7$ K is also well defined. Here, we concentrate only on the interplay between SC and AFM; therefore, all the values extracted from this curve such as the magnetic entropy at 1.5 K (4.8 J/mol K) and the electronic and lattice terms of the $C_p(T)$ will be discussed elsewhere.

Table 1 shows that T_C is more depressed by Pd than by Pt. Therefore, a similar $C_p(T)$ study on $TmNi_{1.9}Pd_{0.1}B_2C$ has been performed, and the results are displayed in Fig. 7. The main effect to be seen is the absence of any magnetic peak down to 0.8 K (the lowest temperature achieved in our equipment) which indicates clearly that Pd ions suppress simultaneously the two critical temperatures T_C and T_N of the system. Possible mechanisms leading to this suppression may be scattering effects, changes in the electronic structure,

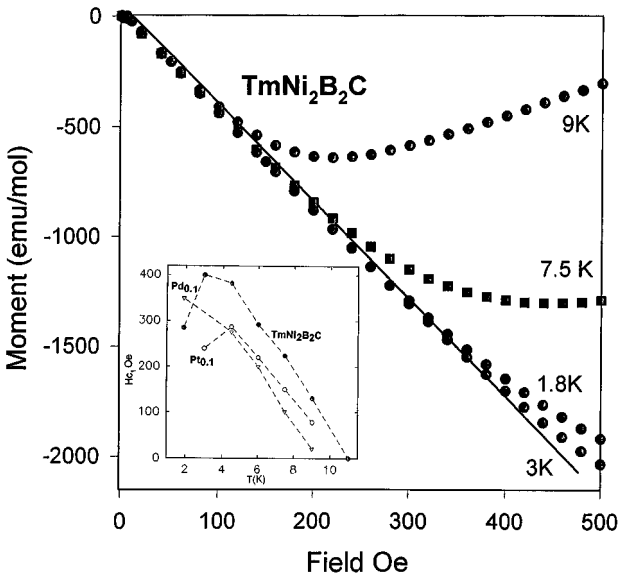

FIG. 5. Low field data of the magnetization curves at various temperatures of $TmNi_2B_2C$. The H_{C1} values for $TmNi_2B_2C$ and $TmNi_{1.9}M_{0.1}B_2C$ (M = Pt and Pd) are shown in the inset Note the decrease at low temperatures.

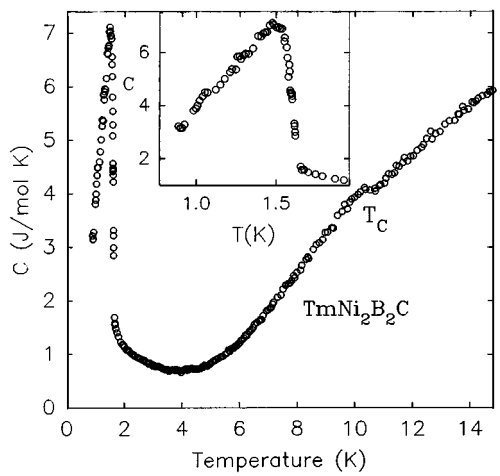

FIG. 6. Specific-heat data measured at $H = 0$ T of $TmNi_2B_2C$. The AFM transition is expanded in the inset.

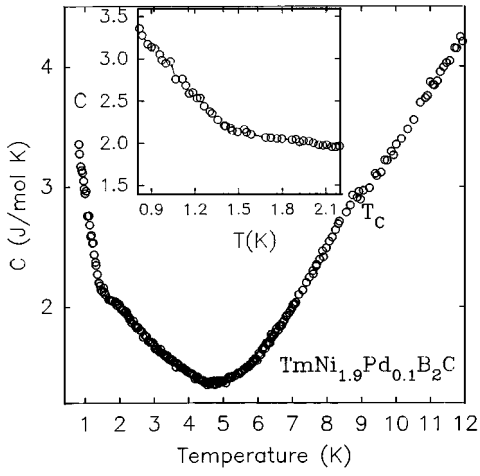

FIG. 7. Specific-heat data measured at $H = 0$ T of $TmNi_{1.9}Pd_{0.1}B_2C$.

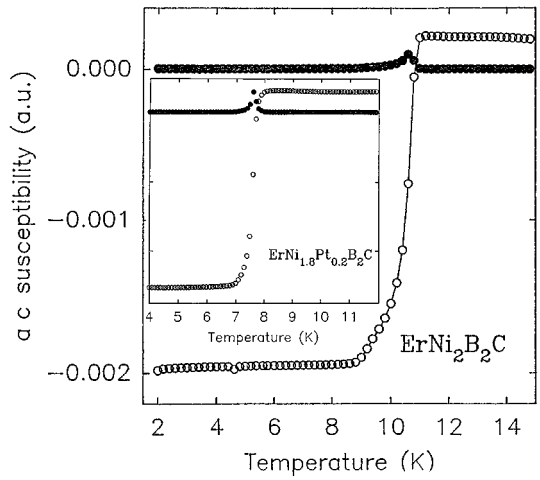

FIG. 8. Ac susceptibility as a function of temperature of $ErNi_2B_2C$ and $ErNi_{1.8}Pt_{0.2}B_2C$.

or expansion in the cell dimension of the doped materials (Table 1). Since pressure measurements on T_C indicate (6) that volume effect due a change in the lattice parameters is negligible for $x < 0.2$, we may speculate that the main reason for the suppression of both critical temperatures is the change in the electronic properties. Magnetic susceptibility measurements performed above T_C show Curie–Weiss behavior in all samples due to the paramagnetic Tm^{3+} ions.

(*B*) *The $ErNi_{2-x}M_xB_2C$ (M = Pd, Pt, and Co) System*

The lattice parameters and the effect of partial substitution in $ErNi_{2-x}M_xB_2C$ on T_C studied by dc susceptibility measurements have been reported recently by Bonville *et al.* (7). The measurements presented here have been performed on the same samples. For undoped $ErNi_2B_2C$, the critical temperatures $T_C = 10.9$ K and $T_N = 6.3$ K are close to each other; therefore the SC transitions for $ErNi_{2-x}M_xB_2C$ were extracted directly from ac susceptibility measurements which are not sensitive to the magnetic nature of the Er sublattice. Figure 8 shows typical ac $\chi'(T)$ and $\chi''(T)$ of $ErNi_2B_2C$ and $ErNi_{1.8}Pt_{0.2}B_2C$, where T_C is defined as the onset of the χ'' curve. The T_C values obtained using the same procedure for all materials studied are listed in Table 1 and compare well with Ref. (7). It appears that, in contrast to the $TmNi_{2-x}M_xB_2C$ system, both Pt and Pd (with the same x) reduce T_C at the same rate.

On the other hand, for the AFM transitions of the Er sublattice, we used the dc SQUID magnetometer at applied fields, higher than the cririca field H_{c2} of the SC state which is $H_{c2}(0) \sim 15$ kOe for $ErNi_2B_2C$ (12). Figure 9 shows the dc $\chi(T)$ curves, measured at 10 kOe, and $T_N = 6.3$ K is defined as the merging temperature of the ZFC and FC branches, where the difference between the branches becomes less than $\Delta\chi = 1 \times 10^{-2}$ emu/mol Oe. This T_N is in perfect agreement with values obtained by other methods (12).

Shown in Fig. 9 (inset) is an expanded view of the dc ZFC and FC curves for $ErNi_{1.8}Pt_{0.2}B_2C$ measured at 40 Oe. The sharp decrease in the two branches below 8 K fits perfectly the onset of the SC state at $T_C = 7.9$ K deduced from Fig. 8. However, irreversibility in the $\chi(T)$ is observed above T_C, and the two branches merge only at 11 K. This irreversibility is related to the AFM structure of the material, which orders at $T_N = 11$ K. Similar behavior is observed in $ErNi_{1.8}Pd_{0.2}B_2C$ and the same critical temperatures were achieved (Table 1). We may conclude that substituting

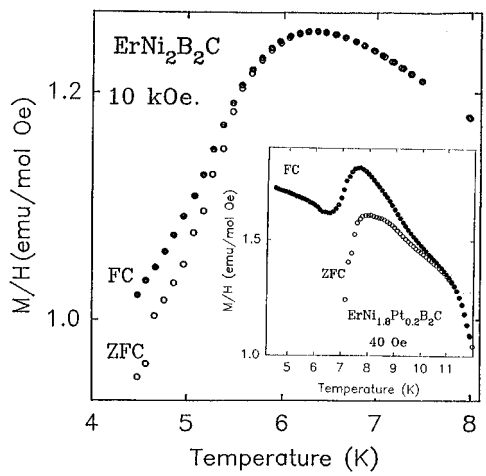

FIG. 9. ZFC and FC susceptibility measured at 10 kOe for $ErNi_2B_2C$, indicating $T_N = 6.3$ K. The inset shows the ZFC and FC susceptibility measured at 40 Oe for $ErNi_{1.8}Pt_{0.2}B_2C$, indicating T_C at 7.9 K and $T_N = 11$ K.

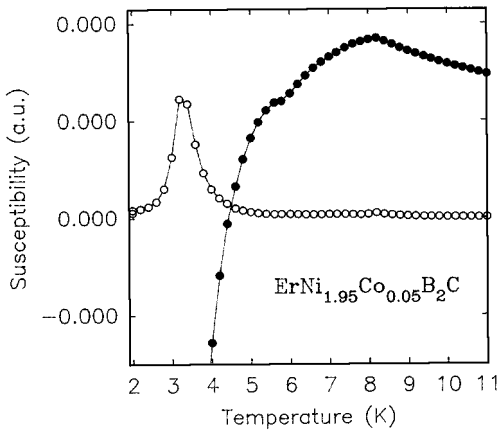

FIG. 10. Ac susceptibility measurements of $ErNi_{1.95}Co_{0.05}B_2C$, showing T_C at 4.8 K and $T_N = 8.2$ K.

isoelectronic Pd or Pt for Ni induces roughly the same volume effect and effect equally T_C and T_N.

The same phenomenon is observed in the $ErNi_{2-x}Co_xB_2C$ system. The ac susceptibility measurements show definitely that for $x = 0.05$ the onset of SC is $T_C = 4.7$ K (Fig. 10). Magnetic studies at elevated temperatures ($T > 15$ K) clearly indicate that the Co ions are not magnetic in these compounds. Therefore, the sharp decrease of T_C is not a result of magnetic pair-breaking. As Co does not carry the same number of valence electron as Ni, we believe that electronic effects are dominant in lowering T_C. Moreover, Fig. 10 shows a peak in the $\chi'(T)$ curve at 8.2 K. This peak is attributed to the AFM ordering of the Er sublattice. The dc measurements confirm this determination. $ErNi_{1.8}Co_{0.2}B_2C$ does not show bulk SC down to 1.9 K, and our dc studies (not shown) indicate that $T_N = 10.9$ K. This means that in the $ErNi_{1.8}M_{0.2}B_2C$ system, the same $T_N = 11(0.1)$K is obtained regardless of M. For $ErNi_{1.5}Co_{0.5}B_2C$ $T_N = 14.8$ K was obtained, indicating that T_N(Er) increases with increasing Co concentration.

4. CONCLUSIONS

In the $TmNi_{2-x}M_xB_2C$ system, dopants such as Pd and Pt reduce both T_C and T_N of the samples. In addition, in the $ErNi_{2-x}M_xB_2C$ system, the common behavior of suppression of T_C by dopants is also obseved. However, here these dopants shift T_N to higher temperatures well above T_C. It appears that the $ErNi_{2-x}M_xB_2C$ system serves as another example of a system in which $T_N > T_C$. The intriguing questions remain as to why the two $TmNi_2B_2C$ and $ErNi_2B_2C$ systems behave differently when they are doped with nonmagnetic elements.

ACKNOWLEDGMENTS

The research was supported by the Israel Academy of Science and Technology and by the Klachky Foundation for Superconductivity.

REFERENCES

1. R. Nagarajan, C. Mazumdar, Z. Hossain, S. K. Dhar, K.V. Gopalakrishnan, L. C. Gupta, C. Godart, B. D. Padalia, and R. Vijayaraghavan, *Phys. Rev. Lett.* **72,** 274 (1994).
2. R. J. Cava, H. Takagi, H. W. Zandbergen, J. J. Krajewski, W. F. Peck, Jr., T. Siegrist, B. Batlogg, R. B. van Dover, R. J. Felder, K. Mizuhashi, J. O. Lee, H. Eisaki, and S. Uchida, *Nature* **367,** 146 (1994).
3. C. Godart, R. Nagarajan, C. Mazumdar, Z. Hossain, S. K. Dhar, K. V. Gopalakrishnan, L. C. Gupta, C. Godart, B. D. Padalia, and R. Vijayaraghavan, *Phys. Rev. B* **51,** 489 (1995).
4. H. Eisaki, H. Takagi, R. J. Cava, B. Batlogg, J. J. Krajewski, W. F. Peck, Jr., K. Mizuhashi, J. O. Lee, and S. Uchida, *Phys. Rev. B* **50,** 647 (1994).
5. Z. Hossain, L. C. Gupta, C. Mazumdar, R. Nagarajan, S. K. Dhar, C. Godart, C. LeviClement, B. D. Padalia, and R. Vijayaraghavan, *Phys. Solid State Commun.* **92,** 341 (1994).
6. H. Schmidt, M. Muller, and H. F. Braun, *Physica C* **235–236,** 779 (1994); H. Schmidt and H. F. Braun, *Physica C* **229**, 315 (1994).
7. P. Bonville, J. A. Hodges, C. Vaast, E. Alleno, C. Godrat, L. C. Gupta, Z. Hossain, and R. Nagarajan, *Physica B* **223–224,** 72 (1996).
8. J. Rohler, *J. Magn. Magn. Mater.* **47–48,** 175 (1985).
9. H. Takagi, R. J. Cava, H. Eisaki, J. O. Lee, K. Mizuhashi, B. Battlogg, S. Uchida, J. J. Krajewski, and W. F. Peck, Jr., *Physica C* **228,** 389 (1994).
10. O. Fischer, *in* "Ferromagnetic Materials" (K. H. Buschow and E. P Wohlfarth, Eds.), Vol. 5, p. 465, (North-Holland, Amsterdam, 1990).
11. B. K. Cho, P. C. Canfield, and D. C. Johnston, *Phys. Rev. B* **52,** 3844 (1995).
12. B. K. Cho, P. C. Canfield, L. L. Miller, D. C. Johnston, W. P. Beyermann, and A. Yatskar, *Phys. Rev. B* **52,** 3684 (1995).